Combined loss of histone methyltransferases GLP and G9a disrupts neural crest cell fate determination

Diana B. Voss, Emily J. Shields, Andrey Poleshko, Li Li, Jun Li, Roger Wang, Mariacristina Calcagno, Rajan Jain*, Cheryl L. Smith*, Jonathan A. Epstein*

Departments of Medicine and of Cell and Developmental Biology, Perelman School of Medicine, University of Pennsylvania, Philadelphia, Pennsylvania 19104

*Co-corresponding authors

3400 Civic Center Blvd

Philadelphia, PA 19104

215-898-4499

epsteinj@pennmedicine.upenn.edu

The authors have declared that no conflicts of interest exist.

Mutations in *EHMT1*, the gene encoding histone methyltransferase GLP, are associated with Kleefstra syndrome (KS), a rare multisystemic disorder with craniofacial and cardiovascular abnormalities (1). The mechanisms by which the loss of histone methyltransferase (HMT) could lead to KS remain poorly understood. *EHMT1*, and its paralog *EHMT2*, which encodes G9a, catalyze the methylation of lysine 9 on histone H3 (H3K9) (2). Given the importance of neural crest to craniofacial and cardiovascular morphogenesis, and the link between GLP mutations and anatomical defects in these neural crest-derived tissues, we sought to assess the impact of HMT loss on neural crest development. We crossed mice in which critical exons of *Ehmt1* and *Ehmt2* were floxed with mice expressing Cre recombinase in pre-migratory neural crest via *Wnt1-Cre* (3). Additionally, $Rosa26^{TdTomato/+}$ was used to lineage trace neural crest derivatives (NCCs, Supplemental Figure 1A).

Expression of GLP and G9a was attenuated at embryonic day 10.5 (E10.5; Supplemental Figure 1B) and undetectable at E11.5 specifically in NCC-derived pharyngeal mesenchyme in GLP/G9a double knockout ("DKO," $Ehmt1^{f/f};Ehmt2^{f/f};Rosa^{TdTomato/+};Wnt1\text{-}Cre+$) embryos compared to control (Figure 1A). Additionally, RNAscope showed reduction of *Ehmt1* and *Ehmt2* mRNA (Supplemental Figure 1C). We observed markedly reduced H3K9me2, but stable H3K9me1 and H3K9me3 levels in NCCs populating the branchial arches and outflow tract in DKO E11.5 embryos (Figure 1A, Supplemental Figure 1D). Isolated NCCs from DKO and control embryos showed persistent reduction of H3K9me2 at E13.5 (Supplemental Figure 1E-F). Thus, GLP and G9a loss in NCCs reduces H3K9me2 but not H3K9me1 or H3K9me3 *in*

vivo. Antibody specificity was confirmed in a peptide competition assay (Supplemental Figure 1G).

Having established GLP and G9a deletion, we investigated their role in NCC morphogenesis. DKO embryos were born at normal Mendelian ratios, but many died perinatally and by postnatal day 14 (P14), no surviving DKO pups were identified (0/30, Supplemental Figure 2A). On P0, DKO pups, unlike controls, showed microcephaly and lacked a milk spot, suggesting they could not suckle (Supplemental Figure 2B-C). All DKO pups also exhibited cleft palates as well as hypoplasia of NCC-derived skull bones (Figure 1B, Supplemental Figure 2D-G). There were, however, no differences in the number of ribs or tibia lengths compared to controls (Supplemental Figure 2H-J).

Given the critical role for neural crest in mediating outflow tract septation and remodeling of the aortic arch arteries, we also examined cardiac morphology. We observed instances of patent ductus arteriosus (PDA; 4 of 5 P0 pups; Figure 1C, Supplemental Figure 2K-M), and double outlet right ventricle with ventricular septal defects (2 of 3 E17.5 embryos, Supplemental Figure 2N) in DKOs but not in controls.

We sought to understand the basis for phenotypes observed in DKOs. We found no differences in the number of NCCs populating the branchial arches, nor in the percentage of proliferating or apoptotic NCCs in E11.5 DKO embryos compared to controls (Supplemental Figure 3A). NCCs normally generate ectomesenchyme-derived bone (4); however, we observed reduced expression of the osteogenic proteins RUNX2 and SP7 in the oral cavity of DKO embryos compared to controls (Figure 1D, Supplemental Figure 3B). NCCs also give rise to some smooth muscle cells surrounding the aortic arch arteries (5). We observed a marked reduction in neural crest-derived cells expressing smooth

muscle actin surrounding the aortic arch arteries in DKO embryos compared to controls (Figure 1E, Supplemental Figure 3C). These data suggest GLP and G9a regulate differentiation of NCCs during craniofacial and vascular development.

To further characterize the impact of GLP and G9a loss on differentiation, we performed RNA-seq on TdTomato+ NCCs isolated from E11.5 branchial arches (Supplemental Figure 4A-C). In comparisons between control and DKO we observed no significant expression differences for gene sets associated with proliferation, apoptosis, or migration (Supplemental Figure 4D). However, analysis revealed significant depletion of neural crest and osteoblast lineage gene sets and enrichment for cardiac muscle, endothelial, and myofibroblast lineage gene sets in DKO relative to controls (Figure 1F, Supplemental Figure 4E-G). Consistent with the expression changes, CUT&RUN from control TdTomato+ NCCs from E11.5 branchial arches revealed significantly higher H3K9me2 signal at genes upregulated in DKOs compared to all genes or DKO downregulated genes (Figure 1G-H). Complementary analysis showed significant enrichment of H3K9me2 at DKO upregulated genes and depletion at downregulated genes relative to random chance (Figure 1I). These results indicate that GLP and G9a loss in NCCs compromises neural crest gene expression and facilitates expression of alternative cell fate pathways. Furthermore, these results suggest that GLP/G9a regulation of H3K9me2 could underlie aspects of craniofacial and cardiovascular defects in some congenital disorders including Kleefstra syndrome.

Funding Support

This work is the result of NIH funding, in whole or in part, and is subject to the NIH Public Access Policy. Through acceptance of this federal funding, the NIH has been given the right to make the work publicly available in PubMed Central.

This work was supported by:

- National Institutes of Health R35HL140018 (to J.A.E.)
- The Cotswold Foundation (to J.A.E.)
- National Institutes of Health R35HL166663 (to R.J.)
- Burroughs Wellcome Foundation Career Award for Medical Scientists (to R.J.)
- WW Smith Charitable Trust (to R.J.)
- National Institutes of Health R21 AG081795 (to A.P.)
- Additional Ventures Catalyst to Independence Award (to D.V.).
- Penn Cytomics is partially supported by the Abramson Cancer Center NCI Grant (P30 016520).

REFERENCES

1. Kleefstra, T., et al., *Loss-of-function mutations in euchromatin histone methyl transferase 1 (EHMT1) cause the 9q34 subtelomeric deletion syndrome.* Am J Hum Genet, 2006. **79**(2): p. 370–7.
2. Tachibana, M., et al., *Histone methyltransferases G9a and GLP form heteromeric complexes and are both crucial for methylation of euchromatin at H3-K9.* Genes Dev, 2005. **19**(7): p. 815–26.
3. Debbache, J., et al., *Cre-driver lines used for genetic fate mapping of neural crest cells in the mouse: An overview.* Genesis, 2018. **56**(6-7): p. e23105.
4. Blentic, A., et al., *The emergence of ectomesenchyme.* Dev Dyn, 2008. **237**(3): p. 592–601.
5. Epstein, J.A., et al., *Migration of cardiac neural crest cells in Splotch embryos.* Development, 2000. **127**(9): p. 1869–78.

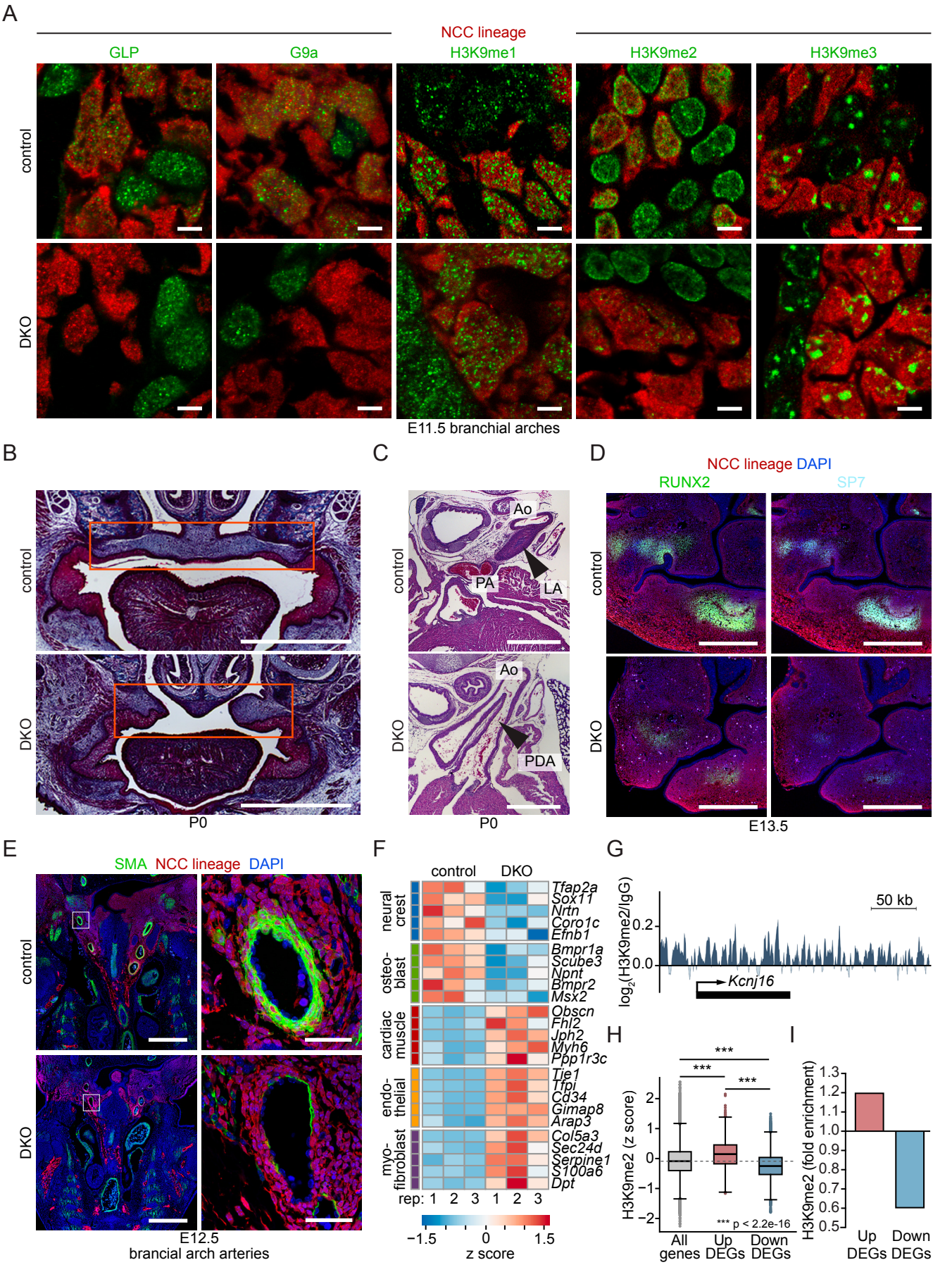
A
NCC lineage
GLP
G9a
H3K9me1
H3K9me2
H3K9me3
control
DKO
E11.5 branchial arches
B
control
DKO
P0
C
Ao
PA
LA
PDA
P0
D
NCC lineage DAPI
RUNX2
SP7
E13.5
E
SMA NCC lineage DAPI
E12.5
brancial arch arteries
F
control
DKO
neural crest
osteo-blast
cardiac muscle
endo-thelial
myo-fibroblast
Tfap2a
Sox11
Nrtn
Coro1c
Efnb1
Bmpr1a
Scube3
Npnt
Bmpr2
Msx2
Obscn
Fhl2
Jph2
Myh6
Ppp1r3c
Tie1
Tfpi
Cd34
Gimap8
Arap3
Col5a3
Sec24d
Serpine1
S100a6
Dpt
rep: 1 2 3 1 2 3
−1.5 0 1.5
z score
G
50 kb
log2(H3K9me2/IgG)
0.2
0.0
Kcnj16
H
H3K9me2 (z score)
***
***
***
*** p < 2.2e-16
All genes
Up DEGs
Down DEGs
I
H3K9me2 (fold enrichment)
Up DEGs
Down DEGs

Figure 1: GLP and G9a loss disrupts neural crest differentiation

(**A**) E11.5 control and DKO embryos immunofluorescence (IF) for TdTomato showing NCC lineage (red), co-stained for GLP, G9a, H3K9me1, H3K9me2 or H3K9me3 (green), scale=5μm.

(**B**) Masson trichrome staining of palatal shelves (box) showing cleft palate in P0 DKO embryo, scale=500μm.

(**C**) H&E P0 sagittal sections with black arrowheads denoting ligamentum arteriosum (LA) in control or patent ductus arteriosus (PDA) in DKO. Ao: aorta; PA: pulmonary artery, scale=500μm.

(**D**) RUNX2 (green) or SP7 (cyan) and TdTomato (red) IF in oral cavity (DAPI, blue), scale=500μm.

(**E**) Smooth muscle actin (SMA) (green) and TdTomato (red) IF of branchial arch arteries (DAPI, blue) [left scale=500μm, right scale=50μm].

(**F**) RNA-seq from E11.5 branchial arch TdTomato+ NCCs shown as heatmaps with 5 of the top 10 genes from lineage-specific gene sets differentially enriched in control or DKO.

(**G-I**) H3K9me2 signal from TdTomato+ NCCs. (G) H3K9me2-enriched gene locus, (H) distributions across all, DKO up- or down-regulated genes (Wilcoxon rank-sum tests, mean of all genes: dashed line, box represents 25-75th percentile range, median is solid horizontal line, whiskers are 10th-90th percentiles), and (I) fold enrichment at DKO DEGs (Genomic Association Tester).